

Application of Inverse and Assimilative Analysis of AMPERE Magnetometer Data



Yining Shi¹, Delores Knipp¹, Tomoko Matsuo¹, Brian Anderson²

¹CU Aerospace Engineering Sciences (ASEN), ²JHU Applied Physics Laboratory (APL)

Overview

We present magnetic potential and FAC response to the **St. Patrick's Day storm of March 2013** using an updated inversion procedure based on Matsuo et al. (2015) with 2-min resolution using magnetic perturbation data from Active Magnetosphere and Planetary Electrodynamics Response Experiment (AMPERE) program.

- **Global snapshots of rapid FACs development during shock passage.**
- **Statistical patterns for FACs response during solar wind sheath passage.**
- **Statistical patterns for FACs response during ICME steady southward Bz interval and comparison to sheath passage.**
- **Global snapshots of strong enhancement in FACs during development of a dawn current wedge.**

Reconstructed Polar Region Magnetic Potential and FAC Patterns

We estimate the magnetic potential and FACs following the optimal interpolation method in Matsuo et al. (2015),

$$\mathbf{x}_a = \mathbf{x}_b + \mathbf{C}_b \mathbf{H}^T (\mathbf{H} \mathbf{C}_b \mathbf{H}^T + \mathbf{C}_r)^{-1} (\mathbf{y} - \mathbf{H} \mathbf{x}_b)$$

$$\mathbf{C}_a = [\mathbf{I} - \mathbf{C}_b \mathbf{H}^T (\mathbf{H} \mathbf{C}_b \mathbf{H}^T + \mathbf{C}_r)^{-1} \mathbf{H}] \mathbf{C}_b$$

\mathbf{x}_b : background mean of the coefficient vector \mathbf{x} ;

\mathbf{C}_b : background model error covariance;

Calculated using ~100 days of magnetic perturbation data provided by the AMPERE program.

\mathbf{y} : AMPERE magnetic perturbation data, +/- 2min interval for each time point;

\mathbf{C}_r : observational error covariance;

\mathbf{H} : linear forward model that maps \mathbf{x} to the observation.

$$\text{Toroidal magnetic potential } \Psi = \Psi \mathbf{x}_a + \epsilon_t$$

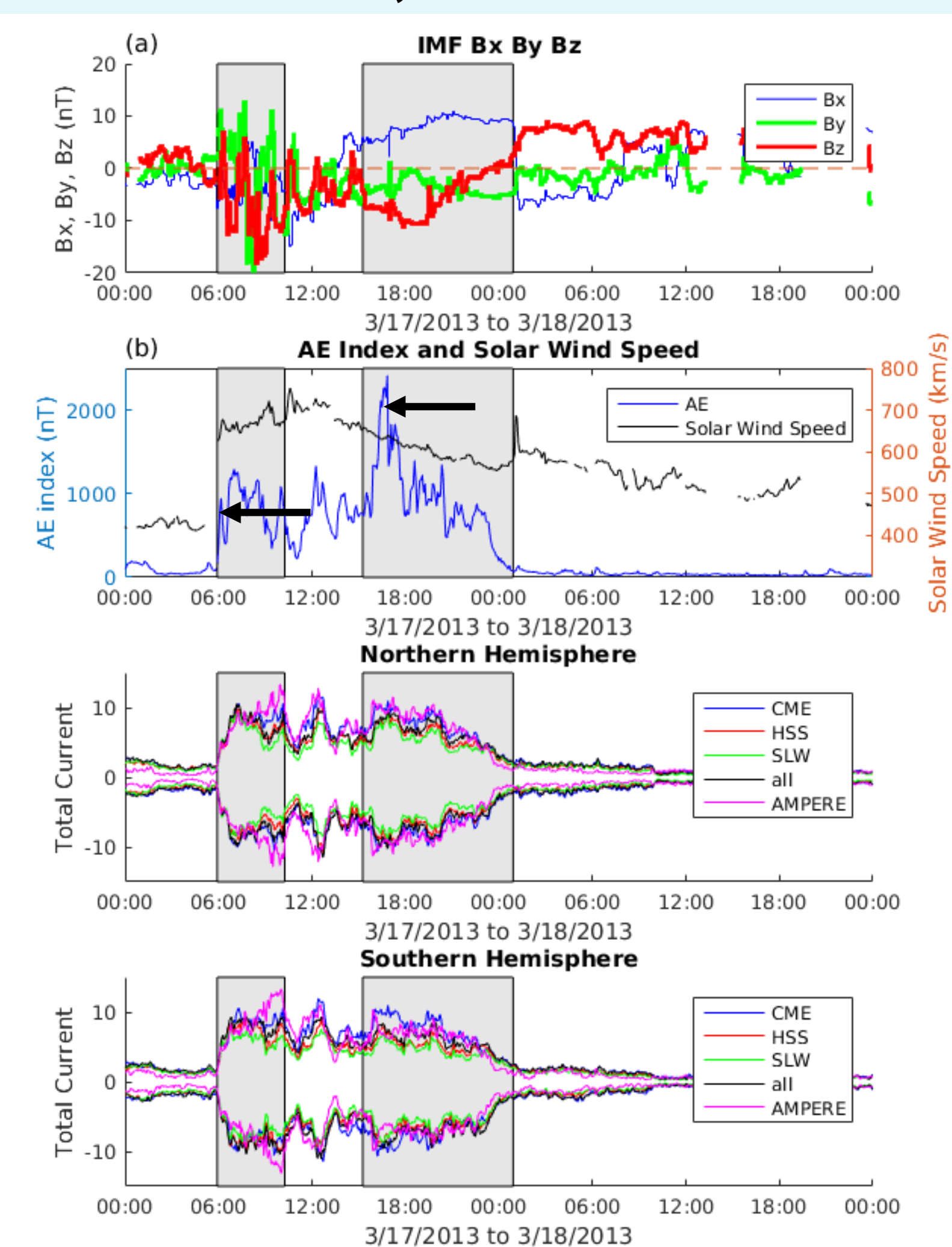
$$\text{FAC } J = \Psi'' \mathbf{x}_a + \epsilon_t$$

Ψ : matrix of polar-cap spherical harmonic basis functions (Richmond and Kamide, 1988);

ϵ_t : truncation error.

Magnetic potential and FAC patterns and corresponding analysis error are estimated with a 2-minute cadence.

March 17th – 18th, 2013 Event

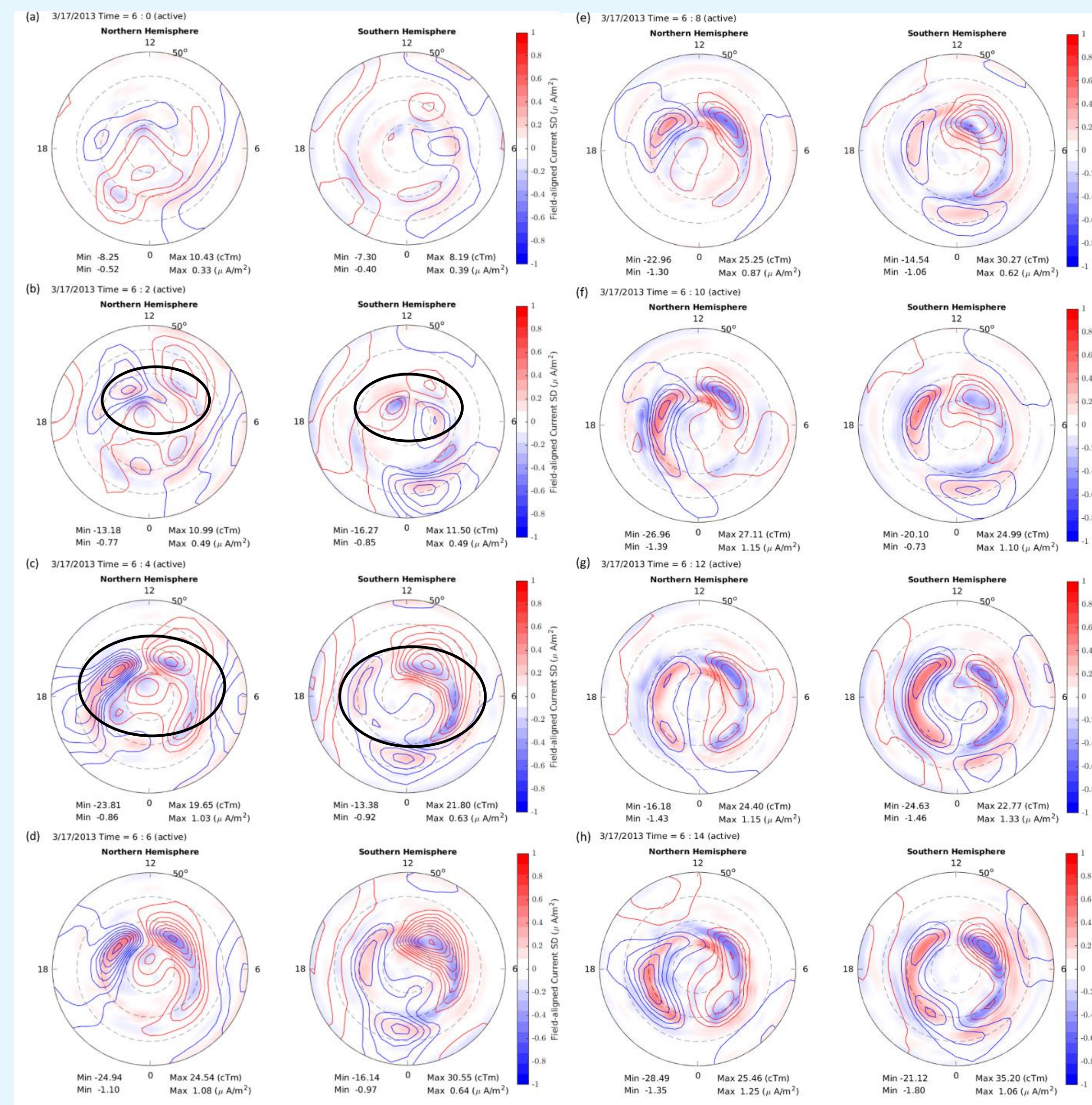


IMF B_x , B_y , B_z , AE Index, solar wind speed, assimilated total currents in two hemispheres with different background models and error covariance matrices and AMPERE total currents for March 17th and 18th, 2013.

Shock passage and entry into solar wind sheath flow 0600 UT to 0614 UT

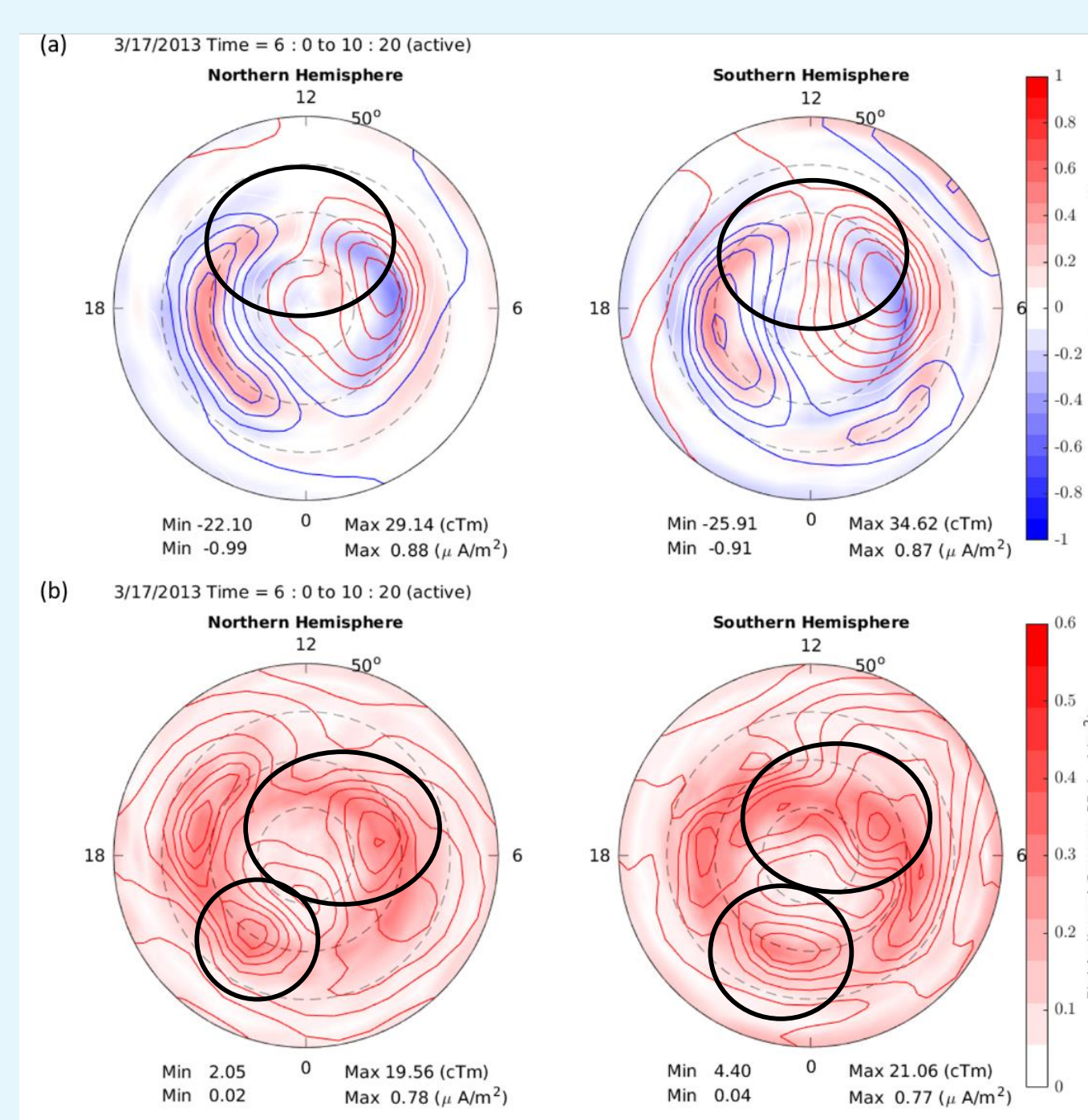
Polar region magnetic potential in line contours and FACs in colors from 0600 UT to 0614 UT each 2 minutes.

- (a) 0600 UT : first weak hints of dayside disturbance
- (b) 0602 UT : clear enhancements in the dayside R0 FACs
- (c) 0604 UT : R1 FAC response develops and propagates tailward
- (d) 0606 UT : disturbance arrives on the nightside
- (g) By 0612 UT : global reconfiguration of the R1/R2 system



Assimilated magnetic potential and FACs from 0600 UT to 0614 UT, showing the FACs response to the interplanetary shock.

Sheath Interval 0600-1020 UT



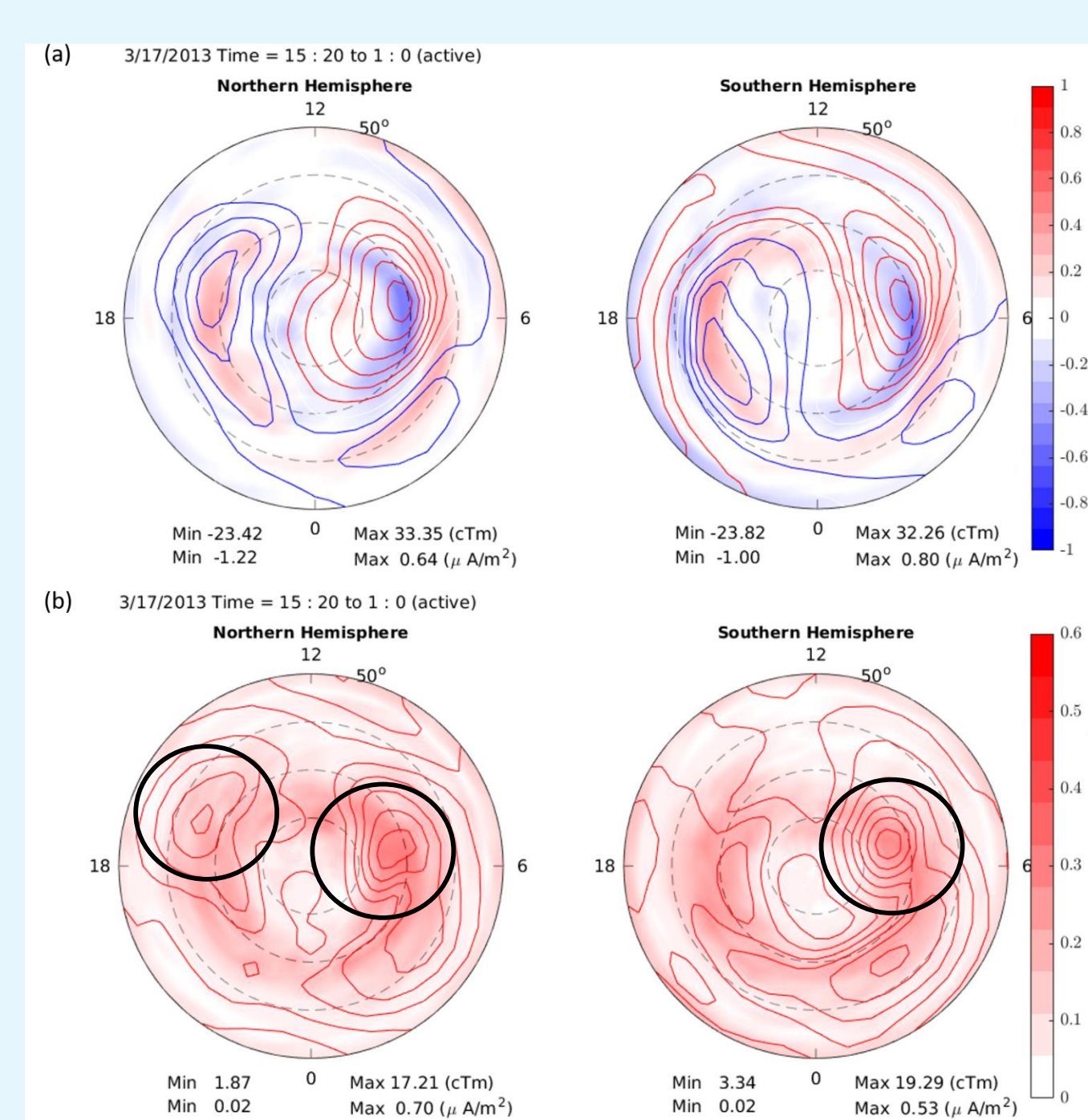
(a) Average:

- R1 currents in noon sector.
- Dawn-dusk asymmetry: stronger on dawnside.

(b) Standard Deviation:

- Dayside and polar cap variation.
- Dawn-dusk asymmetry: stronger on dawnside.
- Strong noon sector variation.
- Pre-midnight variation (substorm).

Southward Bz Interval 1520 – 0100 UT



(a) Average:

- Typical R1/R2 currents
- Dawn-dusk asymmetry: stronger dawnside.

(b) Standard Deviation:

- Weaker variation compared to sheath interval.
- Dawn/dusk side R1/R2 variation.
- Dawn-dusk asymmetry: stronger on dawnside.
- Strong dayside variation.

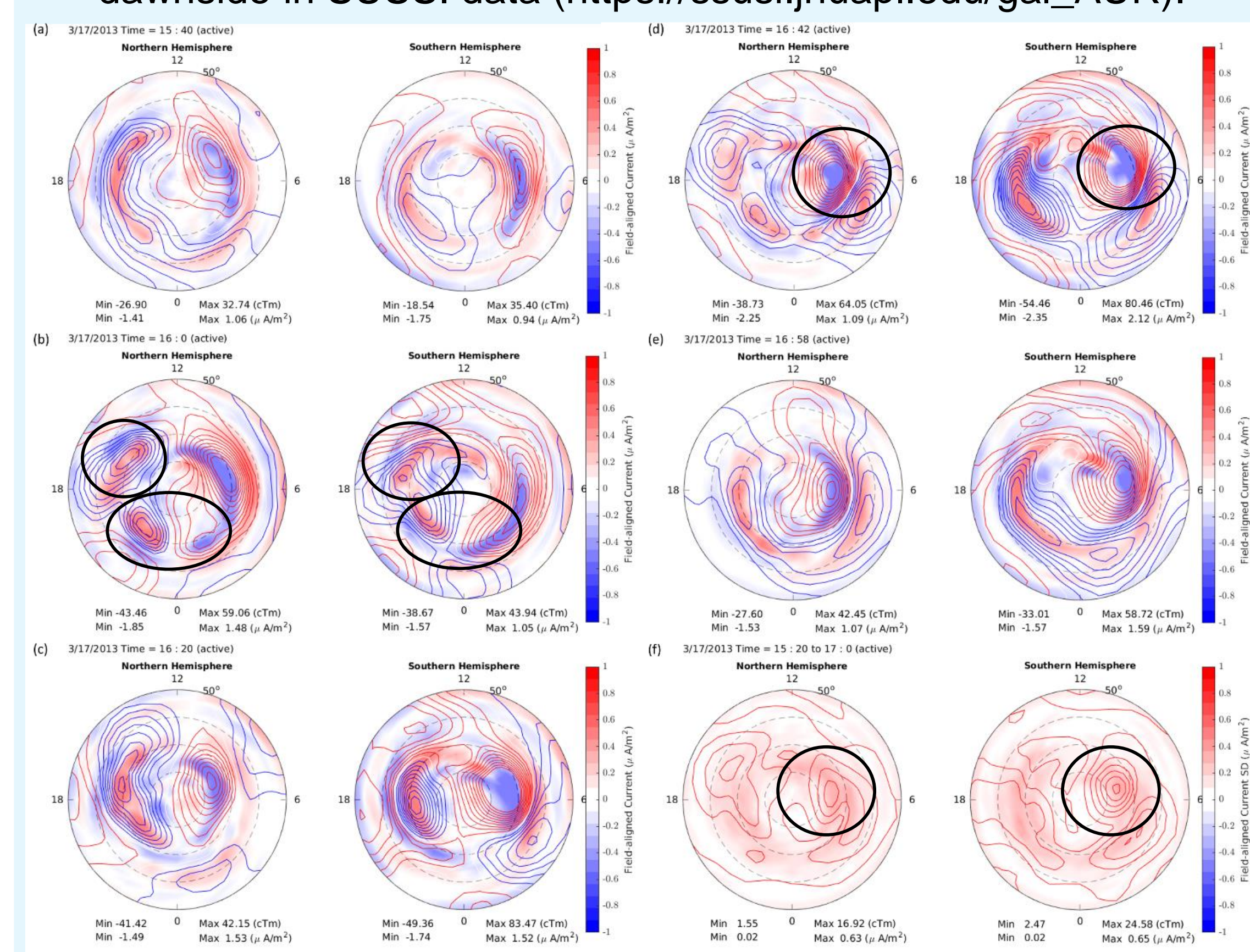
Dawn current wedge event from 1540 UT to 1700 UT

Steady IMF $B_x = 5$ nT, $B_y = -4$ nT and $B_z = -8$ nT for ~80 min.

- (a) 1540 UT : typical FAC configuration
- (b) 1600 UT : mid-afternoon FACs reconfiguration and substorm around midnight
- (c) 1620 UT : intensified FACs near the terminator
- (d) 1642 UT : strong FACs in both hemispheres in the post-dawn region
- (f) Variation from 1540 to 1700 UT : above 70 deg MLT on the sunlit side of the dawn terminator

Additional measurements (not shown):

- Highest AE index reached highest point exceeding 2600 nT at 1651 UT.
- Strong GIC around 1600 UT in IMAGE magnetometer chain located in dusk region (Belakhovsky et al., 2019).
- Enhancement and extension in auroral radiance on the dawnside in SSSI data (https://ssusi.jhuapl.edu/gal_AUR).



Similar phenomenon described in Ohtani et al. (2018): dawnside wedge current system during intense storms.

Conclusions

Updated inversion method to reconstruct high-latitude magnetic potential and FACs.

Event study: March 17th

- Shock passage:** rapid development in dayside FACs and reconfiguration captured.
- Sheath interval:** statistical patterns showing active dayside features and dawn-dusk asymmetry.
- ICME Southward Bz interval:** statistical patterns showing typical R1/R2 current system and dawn-dusk asymmetry.
- Dawn current wedge:** Intense FACs in both hemisphere in the post-dawn region.

Our method provide us the ability to study both rapid FAC response to solar wind drivers with snapshots and statistical patterns.

References And Acknowledgements

We thank the AMPERE team and the AMPERE Science Center for providing the Iridium-derived data products.

Belakhovsky, V., Pilipenko, V., Engebretson, M., Sakharov, Y., & Selivanov, V. (2019). Impulsive disturbances of the geomagnetic field as a cause of induced currents of electric power lines. *Journal of Space Weather and Space Climate*, 9, A18, doi:10.1051/swsc/2019015.

Matsuo, T., Knipp, D. J., Richmond, A. D., Kilcommons, L., & Anderson, B. J. (2015). Inverse procedure for high-latitude ionospheric electrodynamics: Analysis of satellite-borne magnetometer data. *Journal of Geophysical Research: Space Physics*, 120(6), 5241-5251, doi:10.1002/2014JA020565.

Ohtani, S., Gjerloev, J. W., Anderson, B. J., Kataoka, R., Troshichev, O., & Watari, S. (2018). Dawnside wedge current system formed during intense geomagnetic storms. *Journal of Geophysical Research: Space Physics*, 123, 9093-9109, doi:10.1029/2018JA025678.

Richmond, A. D., & Kamide, Y. (1988). Mapping electrodynamic features of the high-latitude ionosphere from localized observations: Technique. *Journal of Geophysical Research: Space Physics*, 93(A6), 5741-5759, doi:10.1029/JA093iA06p05741.